Accepted Manuscript

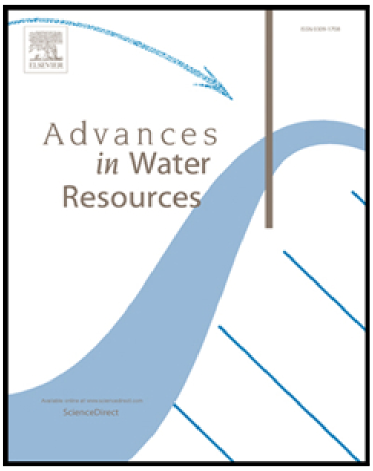

Seasonal and event-based concentration-discharge relationships to identify catchment controls on nutrient export regimes

Camille Minaudo , Rémi Dupas , Chantal Gascuel-Odoux ,
Vincent Roubeix , Pierre-Alain Danis , Florentina Moatar

PII: S0309-1708(18)30616-X
DOI: https://doi.org/10.1016/j.advwatres.2019.103379
Article Number: 103379
Reference: ADWR 103379

To appear in: *Advances in Water Resources*

Received date: 16 July 2018
Revised date: 9 July 2019
Accepted date: 9 July 2019

Please cite this article as: Camille Minaudo , Rémi Dupas , Chantal Gascuel-Odoux , Vincent Roubeix , Pierre-Alain Danis , Florentina Moatar , Seasonal and event-based concentration-discharge relationships to identify catchment controls on nutrient export regimes, *Advances in Water Resources* (2019), doi: https://doi.org/10.1016/j.advwatres.2019.103379

Highlights

- The "C-$Q_{quick\text{-}slow}$" model considers the possibility for concentration-discharge relationships to vary across seasonal and storm event scales
- Nitrate, total phosphorus and soluble reactive phosphorus have contrasting export regimes and often opposite behaviors depending on the time scale
- Diffuse source loading control nitrate seasonal component, and hydrological drivers explain behavior during storms
- Point sources determined phosphorus seasonal amplitudes, and diffuse P sources influenced behavior during storms

Seasonal and event-based concentration-discharge relationships to identify catchment controls on nutrient export regimes

Camille Minaudo[1,2], Rémi Dupas[3], Chantal Gascuel-Odoux[3], Vincent Roubeix[4], Pierre-Alain Danis[5], Florentina Moatar[2,6]

1. Physics of Aquatic Systems Laboratory, EPFL, Lausanne, Switzerland

2. E.A. 6293 GeHCO, University François Rabelais of Tours, Tours, France

3. INRA UMR 1069 SAS, Rennes, France

4. IRSTEA, UR RECOVER, Pôle AFB-Irstea Hydroécologie plans d'eau, Aix-en-Provence, France

5. Agence Française pour la Biodiversité, Pôle AFB-Irstea Hydroécologie plans d'eau, Aix-en-Provence, France

6. RiverLy-IRSTEA, Lyon, France

Corresponding author: camille.minaudo@epfl.ch

Abstract

The analysis of concentration-discharge (C-Q) relationships provides useful information on the processes controlling the mobilization and delivery of chemical elements into streams as well as biogeochemical transformations in river networks. Previous metrics developed to characterize export regimes seldom considered the possibility for the C response to Q dynamics to differ between short-term Q variations during storm events and seasonal Q variations during baseflow periods. Here, we present the "C-$Q_{quick-slow}$" model, which considers the possibility for C-Q relationships to vary across temporal scales. This model was applied in 219 French catchments with various sizes (11 – 2500 km²), land use and hydrological contexts. We evidenced contrasting export regimes for nitrate (NO_3^-), total phosphorus (TP) and soluble reactive phosphorus (SRP), and surprisingly consistent C-Q patterns at the seasonal scale for each parameter. For instance, NO_3^--Q relationships were positive at the seasonal scale in 75% cases and relationships during storms showed either a dilution pattern (24% cases), a non-significant pattern (50%), or a mobilization pattern (12%). TP and SRP relationships with Q at the seasonal scale were almost systematically negative (95%), and patterns during storm events were in most cases mobilization for TP (77%) or non-significant for SRP (69%). We linked the different C-Q relationships with catchment descriptors and found that indicators of diffuse source loading determined NO_3^- seasonal amplitudes, and hydrological drivers could explain the behavior during storms. By contrast, point sources determined P seasonal amplitudes, and diffuse sources controlled P dynamics during storms. The C-$Q_{quick-slow}$ model has the potential to improve nutrient load estimations because of the good predictability of appropriate C-Q archetypes and the possibility to interpolate low frequency concentration data to a daily frequency.

Keywords: concentration-discharge relationships, nutrient export regime, spatial variability; eutrophication, nitrogen, phosphorus, catchment, river network

1. Introduction

The analysis of concentration-discharge (C-Q) relationships provides useful information on the processes controlling the mobilization and delivery of chemical elements into streams (i.e. export regimes) as well as biogeochemical transformations in river networks (Bieroza et al., 2018; Godsey et al., 2009; Moatar et al., 2017; Musolff et al., 2017, 2015). Export regimes have been classified as chemostatic, when concentrations vary little compared to discharge, or chemodynamic, when concentrations variability is larger (Musolff et al., 2015). Export regimes have generally been interpreted in terms of spatial distribution of sources in three spatial dimensions: vertically in depth (Abbott et al., 2018; Dupas et al., 2016; Musolff et al., 2016), laterally along hillslopes (Musolff et al., 2017) and longitudinally from upstream to downstream reaches (Dupas et al., 2019a, 2017; Tiwari et al., 2017). Homogeneously distributed sources mainly lead to chemostatic export regimes whereas heterogeneously distributed sources mainly lead to chemodynamic export regimes (Basu et al., 2011; Dupas et al., 2016; Godsey et al., 2009; Moatar et al., 2017; Musolff et al., 2015). Temporally variable biogeochemical reactions in terrestrial and aquatic ecosystems may also enhance or attenuate the chemostatic and chemodynamic character of export regimes (Minaudo et al., 2015).

Different metrics and thresholds have been used to characterize export regimes. On the one hand, several authors have compared the coefficient of variation of concentration (CVc) to the coefficient of variation of discharge (CVq) (Dupas et al., 2019b; Musolff et al., 2017, 2015; Thompson et al., 2011; Underwood et al., 2017) or investigated the so-called “temporal Lorenz inequality” (Gini coefficients, Jawitz & Mitchell, 2011; Williams et al., 2016). On the other hand, other authors have used the slope of C-Q relationships in logarithmic domain as a metric of export regimes: if the slope coefficient is non-significantly different from zero, the export regime is considered chemostatic, while slopes significantly different from zero characterize a chemodynamic export regime (Ameli et al., 2017; Basu et al., 2011; Diamond and Cohen, 2018; Godsey et al., 2009; Kim et al., 2017; Koenig et al., 2017; Moatar et al., 2017). This second approach allows not only to characterize export regimes as chemostatic and chemodynamic, but also to describe observed patterns as dilution, constant and mobilization archetypes (Musolff et al 2017). However, fitting a single linear regression on C-Q plots is sometimes questionable due to large dispersion in C-Q plots (even log transformed). Many factors cause this dispersion: i) hysteresis and non-linearity effects due to source and transport limitations (Benettin et al., 2017); ii) instream biogeochemical transformations on nutrient concentration without temporal correlation with hydrological variations (Bieroza and Heathwaite, 2015; Moatar et al., 2017); iii) seasonal and long-term variations in C-Q relationships (Hirsch, 2014; Zhang et al., 2016).

This dispersion in C-Q plots is a manifestation of ambivalent situations where the same Q corresponds to different ecohydrological conditions in the catchment, and thus produces different C (Bol et al., 2018). Ambivalent situations have been highlighted by several authors who found opposite C-Q patterns (dilution versus mobilization) at seasonal and storm event time scales (Duncan et al., 2017a; Dupas et al., 2017; Li et al., 2019) possibly leading to zero C-Q slopes on average although both seasonal and storm event slopes were significantly different from zero. Figure 1 is an illustrative example showing two C-Q relationships subject to high dispersion effects. In these examples, discharge during a summer storm event is comparable with discharge during winter baseflow, but ecohydrological conditions differ considerably, leading to different concentrations. Nitrate tended to be highest during winter baseflow (observation A), whereas P tended to be highest during a summer storm event (observation D). These examples suggest that considering both slow and quick flow components has the potential to improve C-Q models, and this is the main hypothesis of this paper.

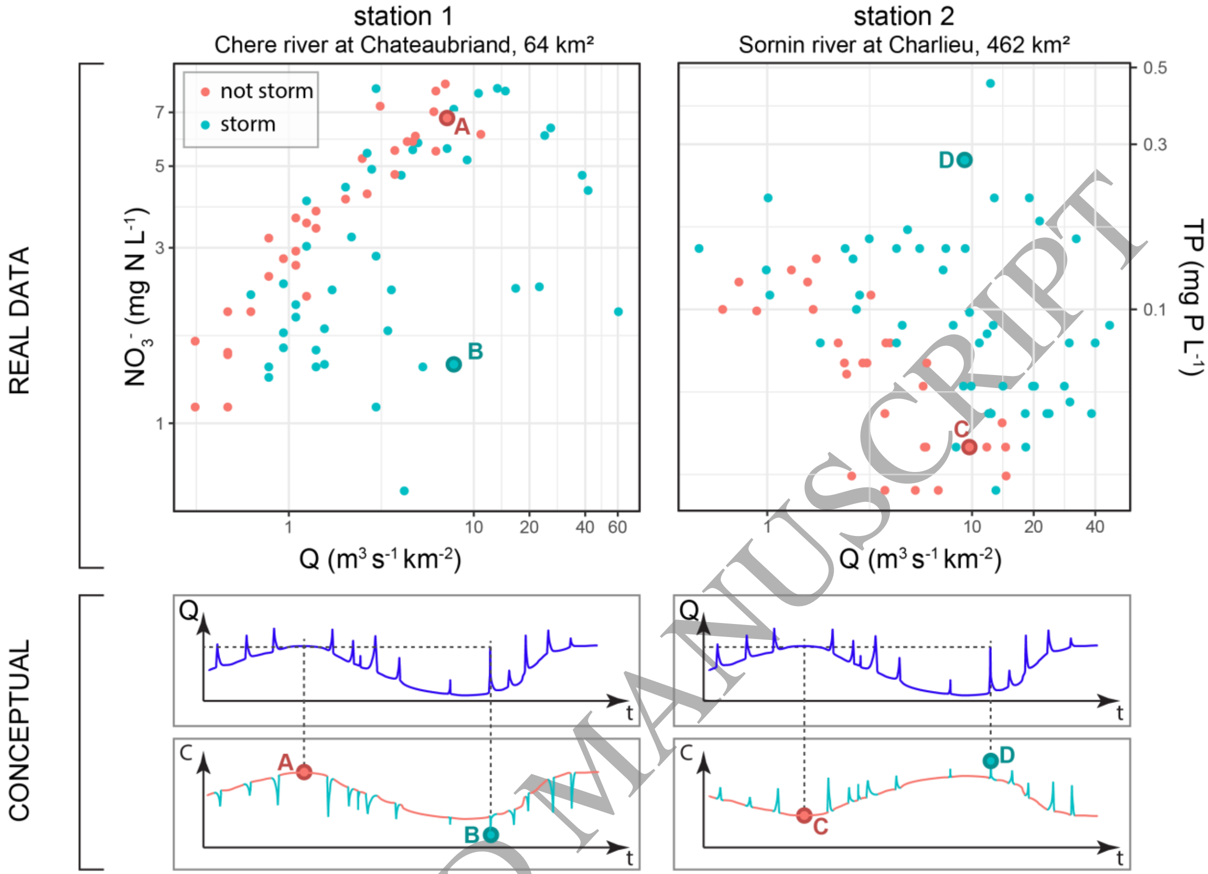

Figure 1. Concentration response to discharge fluctuations highly depends on the hydrological conditions (not only the value of discharge but also whether discharge is subjected to quick or slow variations). Top row: C-Q relationships at two stations located in France (left: nitrate, right: total phosphorus). Measurements during storm events were differentiated from the rest of the observations based on hydrograph separation (see section Method for details and data sources). Bottom row: Hypothetical responses of C to seasonal and storm event Q variations.

These examples also show that C observations during storm events overlap with values measured during baseflow periods. Therefore, splitting the C-Q diagram based on a percentile of discharge (Diamond and Cohen, 2018; Moatar et al., 2017) does not necessarily separate storm events from seasonal variations, and cannot possibly solve the dispersion effect commonly observed in C-Q plots. The approach developed in the WRTDS model (Weighted Regression on Time, Discharge and Season, Hirsch, 2014; Zhang et al., 2015; Zhang, Harman, et al., 2016; Zhang & Ball, 2017) addresses most of the dispersion issues listed above, and efficiently interpolates low-frequency time series. Unfortunately, the WRTDS model includes four parameters and therefore cannot be considered a parsimonious approach. These coefficients are calibrated at each time step, which makes difficult to interpret what drives the heterogeneity often observed in terms of catchment behavior.

This guided us towards the formulation of a double C-Q relationship, the model named hereafter "C-$Q_{quick\text{-}slow}$", which enables seasonal (slow) C-Q slopes to differ from storm event (quick) C-Q slopes. Firstly, we assessed the skills of our C-$Q_{quick\text{-}slow}$ model to fit observations and characterize nutrient export regimes at both temporal scales. Secondly, we explored the spatial variability of the different C-Q archetypes encountered across diverse physical and ecological contexts. We expected variability in these C-Q relationships to be primarily controlled by land use and hydrological flow paths. To test this hypothesis, we established statistical links between a set of catchment descriptors (e.g. land use cover, and morphological, hydrological and geological attributes) and the C-$Q_{quick\text{-}slow}$ model parameters. This was achieved using a large database comprising 219 independent catchments (11 to 2500 km²) where nitrate, total phosphorus and soluble reactive phosphorus concentrations have been monitored monthly, and discharge measured daily, within a French national program for water quality monitoring over the period 2008-2015.

2. Material and methods

2.1. C-Q analysis

We assumed that C-Q relationships are the combination of the C response to seasonal (slow) Q variations with the C response to storm-event (quick) Q variations, and this constituted the essence of the "C-$Q_{quick\text{-}slow}$" model. It does not necessarily mean that Q variations are the cause of C variations, but only that they covary or anti-covary in time. The seasonal and storm event variations in discharge were estimated from hydrograph separation into slow and quick components (Equation 1).

$$C(t) = \beta_0 + \beta_1 \cdot log\big(Q_{slow}(t)\big) + \beta_2 \cdot log\left(Q_{quick}(t)\right) + \varepsilon \qquad \text{Equation 1}$$

where all β_i are adjusted coefficients, and ε represents the residuals.

To estimate Q_{slow} and Q_{quick}, we normalized discharge by interannual median flow, and used the baseflow recursive filter method (Lyne and Hollick, 1979; Nathan and McMahon, 1990) with 3 passes and a filter parameter set at 0.925. This method separates total flow into a seasonal component and a short-term component called hereafter "storm event" in the manuscript. Seasonality of the "slow" component was verified by computing autocorrelation curves of Q_{slow} at all sites (Figure S.1 in Supplement file).

Model outputs consisted in the fitted coefficients $\beta_0, \beta_1, \beta_2$ and performance indicators: the root mean squared error normalized by the standard deviation of observations (*nRMSE*), adjusted explained variance (*R²_adj*), and p-values for each coefficient in Equation 1. A linearity test was computed on residuals to verify that 95% of studentized residuals lied within the interval [-2, 2].

For both the seasonal and the storm event scales, the relationship between C and Q variations could either be positive (covariation, or mobilization), negative (anti-covariation, or dilution) or non-significant (chemostasis for nearly constant C, or neutrality when C variations exist that are not driven by Q fluctuations). We considered a relationship to be non-significant when the associated p-value exceeded 0.05. The sign of the C-Q relationship at the seasonal scale (β_1) could be different from the sign of the C-Q relationship at the storm event scale (β_2). Thus, three possibilities (negative, non-significant, and positive) for two temporal scales (slow and quick) led to consider that only 9 different C-Q archetypes theoretically exist.

2.2. Dataset for C-Q analysis

Water quality parameters included in this analysis were nitrate (NO_3^-), total phosphorus (TP) and soluble reactive phosphorus (SRP). Concentrations were measured on grab samples collected for physico-chemical analysis every other month on average. Across approximately 10,000 water quality stations present in the French national public database (http://www.naiades.eaufrance.fr/), we selected stations meeting all the following criteria: i) C station can be paired with a Q station (data from http://www.hydro.eaufrance.fr/) when their catchments share at least 90% surface area; ii) all C catchments are independent; iii) C data contains at least 50 observations after outliers removal (i.e. values over 200 mgN L^{-1} and 5 gP L^{-1}) over the period 2008-2015; iv) at least 30% of C observations occurred during "major" hydrological events (defined here as $Q(t) > 1.5 \times Q_{slow}$); v) trends on C are non-significant over the period (p-value of Sen's Slope test > 0.05, following Hipel and McLeod (2005)) to avoid penalizing the model. Finally, stations where a single concentration value was observed more than 15% of the time were removed from the selection, a situation often seen in P surveys when concentrations are below quantification limits. This resulted in 219 catchments with respectively 179, 138 and 107 individual time series for NO_3^-, TP and SRP.

2.3. Relationships with catchment descriptors

The selected catchments encompassed contrasting physical contexts in terms of morphology, nutrient diffuse and point sources, and hydrological and geological properties (see Table 1 and Figure 2 for data description). Catchment size ranged from 11 to 2500 km², with 87% of catchments <500 km². Approximately 55% of the catchments had at least 1/3 of their total area covered by arable land (p_arable), indicating potentially high N and P surplus and thus stream water quality likely to be significantly impacted by diffuse agricultural sources. Most catchments received limited N and P point sources (only 10% received over 10 kg N ha^{-1} y^{-1}, and only 2% received over 0.1 kg P ha^{-1} y^{-1}). Lithological contexts included both sedimentary and crystalline bedrocks dominancy as shown by bimodal density plot on the percentage of catchment over a sedimentary bedrock (p_sedim on Figure 2). Hydrological descriptors covered a large climatic gradient: mean ± standard deviation of effective rainfall, base flow index (BFI) and index of hydrological reactivity (W2) (descriptions in Table 1) were respectively 700 ± 160 mm y^{-1}, 55 ± 9 and 17 ± 5%.

We investigated the link between fitted coefficients of the fitted C-$Q_{quick\text{-}slow}$ model with a set of catchment descriptors (Table 1 and Figure 2), using Pearson correlation coefficients (assuming linear relationships) and associated p-values. We considered correlations as significant when p-value < 0.05. We conducted this correlation analysis on a subset of C-Q fitted coefficients that exhibited reasonable goodness of fit (*nRMSE* < 200%).

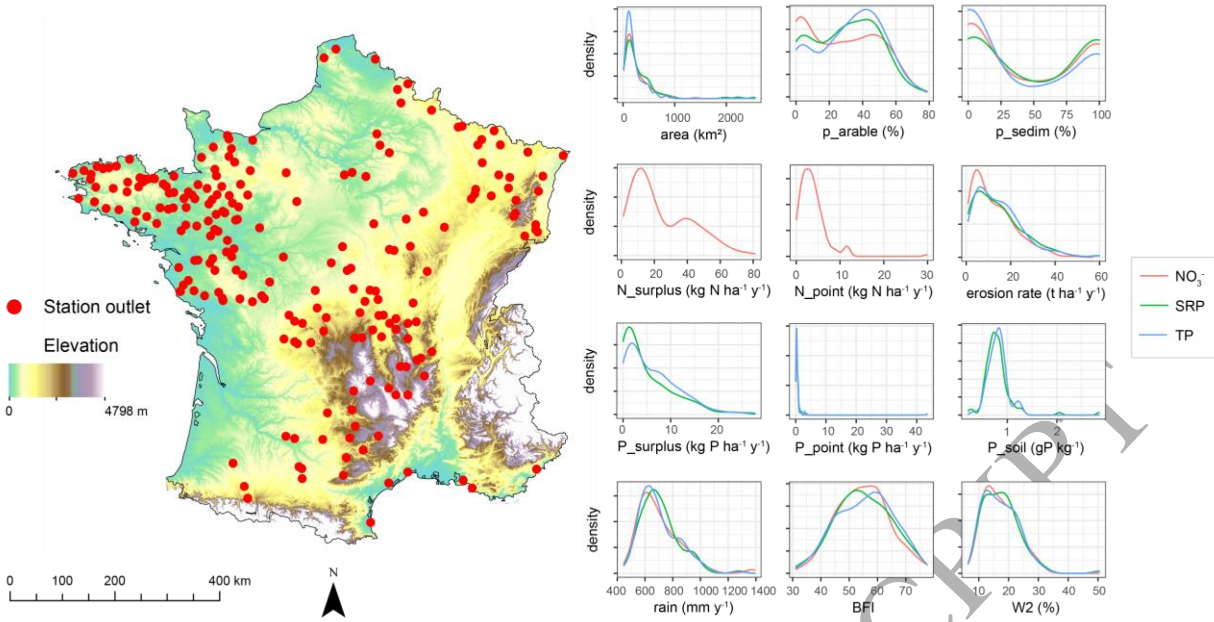

Figure 2. Monitoring stations for analysis and density plots of their catchment descriptors (see Table 1 for descriptors' definitions).

Table 1. List of catchment descriptors included in the analysis, and associated sources.

Descriptor type	Variable name	Unit	Definition	Source
Morphology	area	km²	Catchment area	http://www.naiades.eaufrance.fr/
Diffuse and point N and P sources	N_surplus P_surplus	kg N ha^{-1} y^{-1} kg P ha^{-1} y^{-1}	Surplus of nitrogen and phosphorus	NOPOLU model. Doublet & Le Gall (2013); Snoubra (2013); (Dupas et al., 2015a)
	N_ point P_point	kg N ha^{-1} y^{-1} kg P ha^{-1} y^{-1}	Nitrogen and phosphorus loads of domestic and industrial point sources	http://assainissement.developpement-durable.gouv.fr/services.php http://www.eau-loire-bretagne.fr/informations_et_donnees
	P_soil	g P kg^{-1}	Total phosphorus soil content	Delmas et al., (2015)
Soil erosion	erosion	t ha^{-1} y^{-1}	Erosion rate derived from land use, topography and soil properties	Cerdan et al., (2010)
Hydrological indicators	precipitation	mm y^{-1}	Average effective rainfall, calculated as P-ETP for the months when P-ETP > 0	SAFRAN database, Quintana-Segui et al., (2008)
	BFI	-	Base flow index	Eckhardt (2008)
	W2	%	Index of hydrological reactivity representing the percentage of total discharge that occurs during the highest 2% flows	Moatar et al., (2013)
Land use	p_arable	%	Percentage of arable land	Corine Land Cover (2006)
Geology	p_sedim	%	Percentage of sedimentary rocks derived from simple lithological maps	LITHO database (2008)

All analyses were conducted with R (R Core Team, 2016) with 'EcoHydRology', 'lubridate', 'hydroGOF', 'trend', 'GGally' and 'ggplot2' packages.

3. Results

3.1. C-Q model performances

The *nRMSE* was under 200%, for 81%, 78% and 65 % of catchments for NO_3^-, TP and SRP, respectively (Figure 3). The median *R²_adj* value was 0.39, 0.28 and 0.30 for NO_3^-, TP and SRP, respectively, and 10th percentile – 90th percentile ranges of *R²_adj* were 0.12-0.63, 0.11-0.43, and 0.07-0.60. Approximately 80% of model fits passed the linearity test (results not shown). In the examples of Figure 3, seasonal variations were well reproduced, and concentration dynamics during short term storm events seemed to be correctly modeled for both dilution and mobilization processes, even if some storm events were sometimes underestimated. C-Q behaviors in a logscale C-Q diagram showed contrasting patterns, and dispersion in these plots varied depending on which component (slow or quick) dominated the total flow.

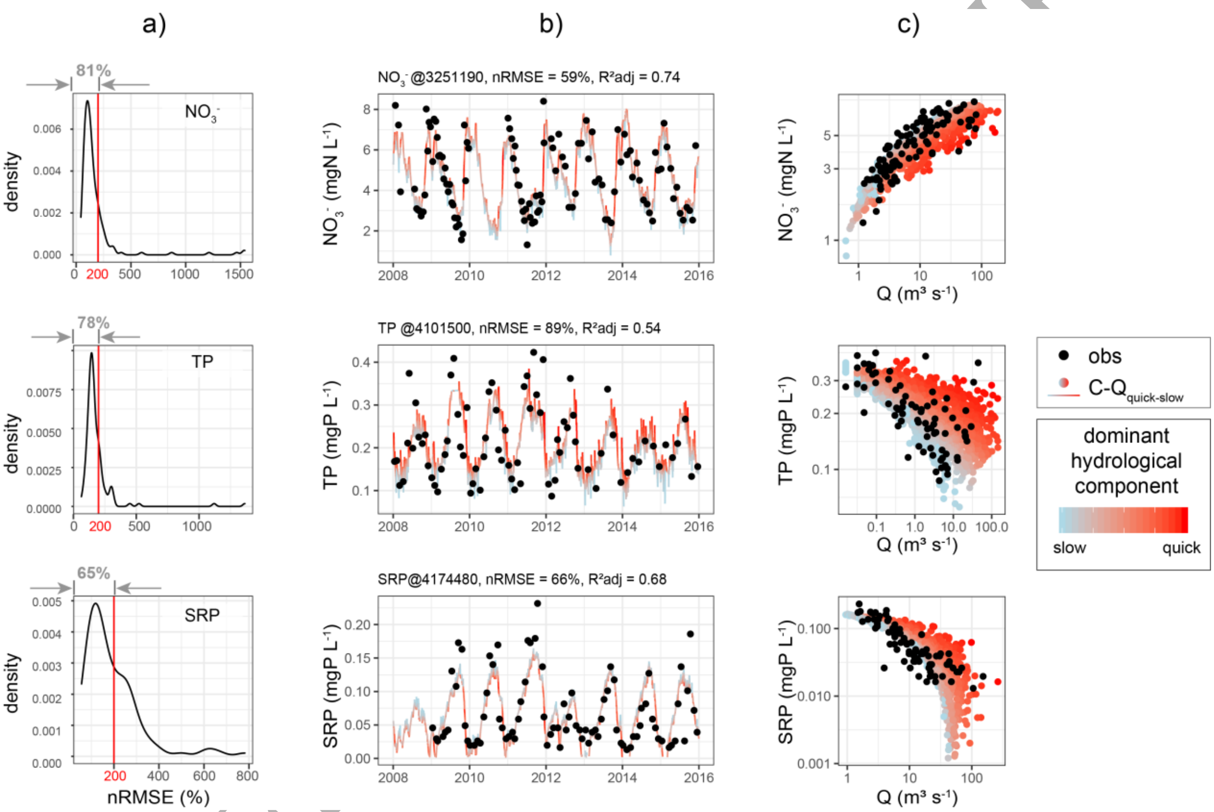

Figure 3. a) C-Q fits performances (*nRMSE* density plots) at all stations. Red vertical lines indicate *nRMSE* =200%. Grey percentages above density plots indicate the proportion of stations with *nRMSE* under 200%.; b) examples of C-Q fits for NO_3^-, TP and SRP at three different stations and c) depicts the same observed and modelled concentrations in more classical logscale C-Q plots.

3.2 C-Q typologies for N and P

Interestingly, only 2 or 3 C-Q archetypes among the nine possibilities were observed for each parameter (Figure 4). For NO_3^-, the seasonal component covaried positively in most cases with baseflow seasonality ($\beta_1 > 0$ for 86% of the catchments), and the dynamics during storm were either non-significant (52% cases), showing a dilution pattern ($\beta_2 < 0$, 28% of cases), or a mobilization pattern ($\beta_2 > 0$, 20%). Thus, the most represented archetype was a positive C-Q slope at the seasonal scale combined with a non-significant storm component (50% cases).

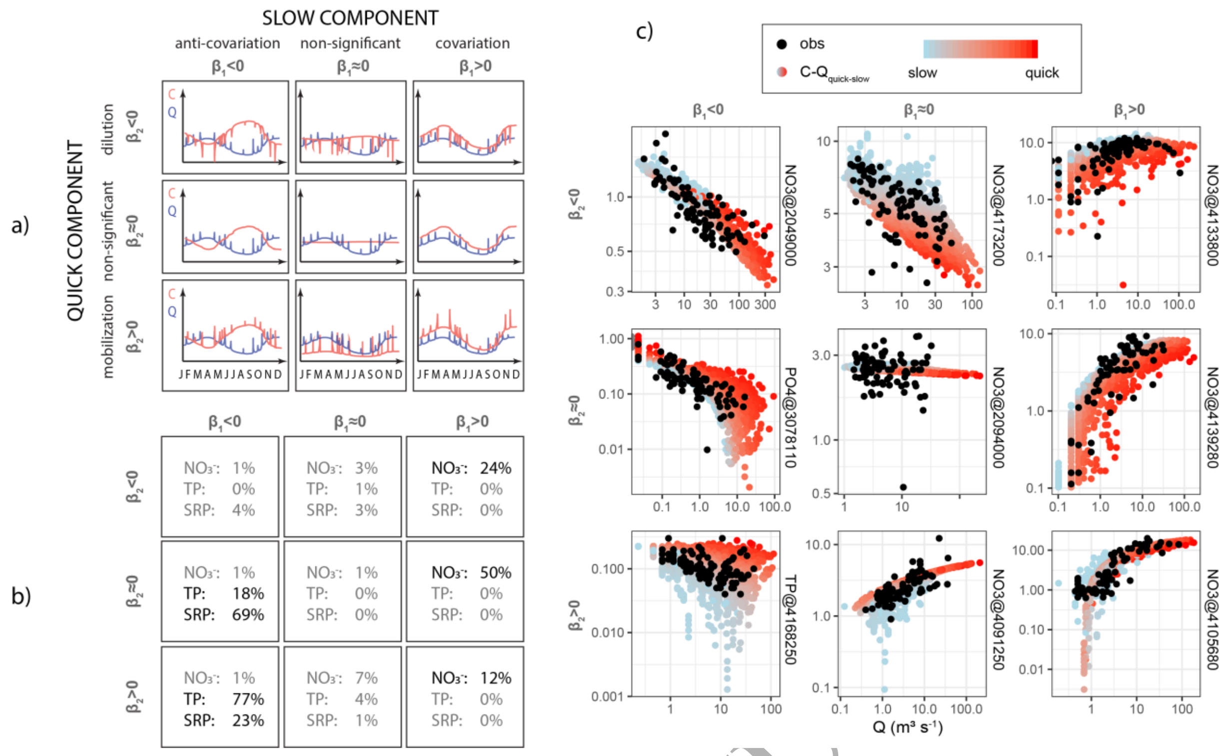

Figure 4. a) conceptual daily evolutions over one year for C and Q based on the nine potential C-Q archetypes, b) proportions of C-Q archetypes encountered in our database for NO_3^-, TP and SRP for catchments where *nRMSE* < 200%. Numbers in black highlight archetypes encountered in more than 10% occurrences, and c) examples of logscale C-Q plots for each of these 9 possibilities.

For TP, 95% of catchments displayed seasonal variations opposite to baseflow seasonality ($\beta_1 < 0$). The remaining 5% presented a non-significant seasonal component. The TP dynamics during storm events were a mobilization pattern in most cases ($\beta_2 > 0$ for 81%), and the remaining 19% presented non-significant dynamics during storms. The most represented C-Q archetype for TP was a negative C-Q slope at the seasonal scale, combined with a mobilization storm component (77%). For SRP, seasonality was similar to TP, i.e. a negative C-Q slope at the seasonal scale for 96% of the catchments ($\beta_1 < 0$). Compared to TP, a larger proportion of catchments presented a non-significant storm event component. This concerned 69% catchments and represented the most observed C-Q archetype as 23% presented a mobilization pattern and only 4% a dilution pattern.

These nine different C-Q archetypes were highly contrasted when presented in a classic logscale C-Q diagram (Figure 4c). Dilution or mobilization patterns were clearly represented and dispersion in the plots depended on which component (slow or quick) dominated. Points corresponding to a quick component dominating the total flow were found on top or bottom of the cloud of points depending on the sign of β_2. As expected from our C-Q model design, negative β_2 produced a larger dispersion towards lower C values, and positive β_2 produced a larger dispersion towards higher C values.

3.2. Linking C-Q relationships with catchment descriptors

The link between C-Q fitted coefficients calibrated with Equation 1 and a set of catchment descriptors was assessed based on linear Pearson correlations. We computed correlation values for the C-Q types encountered more than 10% of the time in the database (section 3.1).

The coefficient β_0 represented the background pollution, β_1 was associated with seasonal variations, and β_2 the variations in storms.

For NO_3^- (Figure 5), the background pollution β_0 was highly correlated with diffuse agricultural sources (R correlation coefficients ranged from 0.6 to 1 with N surplus and the proportion of arable land in the catchment) for all C-Q types identified. The seasonal component β_1 was highly linked with β_0 (correlation was over 0.9), indicating larger seasonal magnitude in the most polluted catchments. The magnitude of the storm component β_2 was linked to diffuse sources: significant correlation coefficients were found between β_2 and p_arable, N surplus, and erosion rate depending on the C-Q type. Hydrological descriptors, erosion rate and lithology classes differentiated the catchments presenting contrasting C-Q archetypes: dilution patterns in storms ($\beta_2<0$) were associated with high BFI values, low W2 values, low values of erosion rate and mostly located on crystalline bedrock. By contrast, mobilization patterns in storms ($\beta_2>0$) were associated with catchments presenting low BFI, high W2 and high erosion rate, and mostly located on sedimentary rocks.

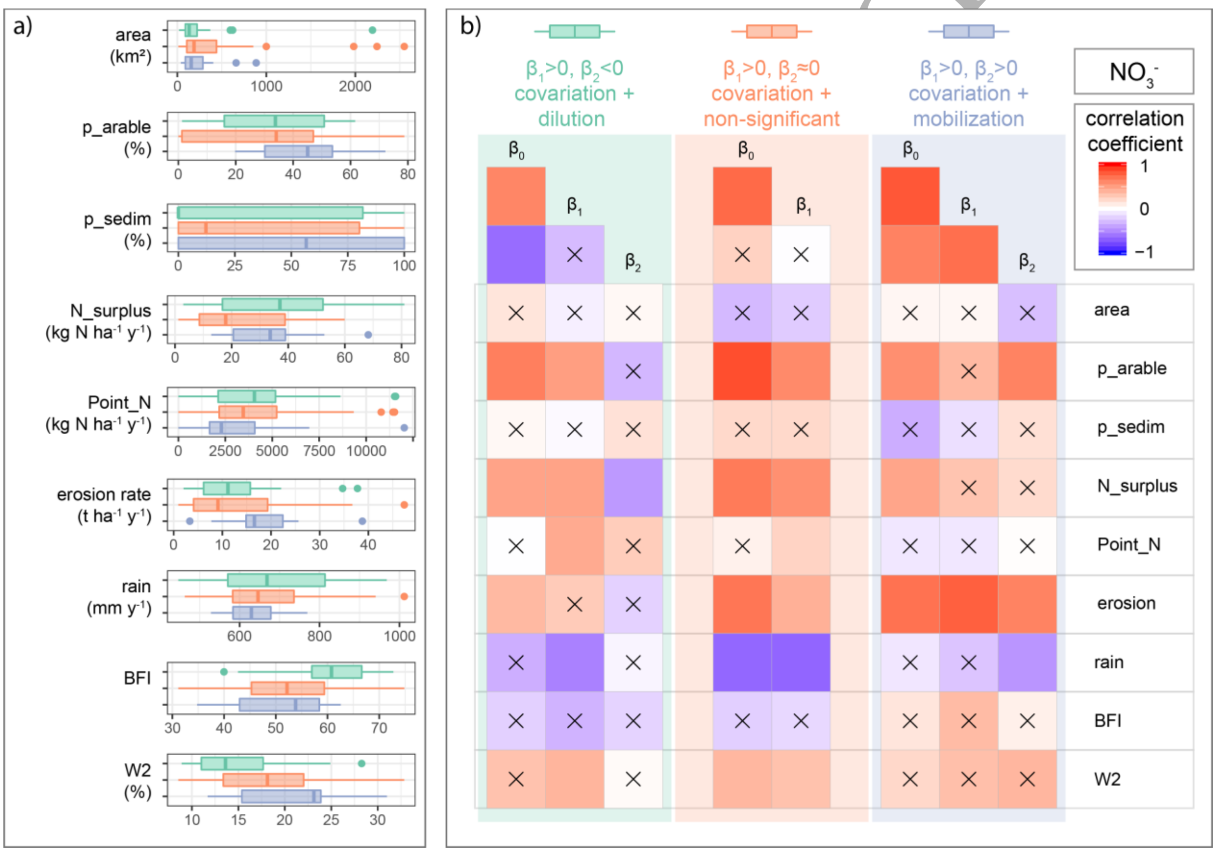

Figure 5. Ranges (a) and correlation matrices (b) between C-Q features (selection based on nRMSE < 200%) characterized by NO_3^- background pollution (β_0), seasonal C-Q (β_1), storm C-Q (β_2) and catchment descriptors for the most represented NO_3^--Q types (more than 10% occurrences). Black crosses indicate non-significant correlations. Pearson correlation coefficients among catchment descriptors can be found in Table S.1 in the Supplement file.

For TP (Figure 6), the coefficient β_0 was highly and positively correlated with point P sources (R was 0.6 to 1). Seasonal dynamic was always opposite to the baseflow Q seasonality ($\beta_1<0$) (Figure 4). The amplitude of the seasonal component β_1 was clearly anti-correlated with P point sources (R was -1 to -0.8). We found that, compared to catchments where behavior in storms was not significant, catchments with significant mobilization storm event component presented higher ranges of P surplus, soil P content, erosion rate, effective rainfall, and BFI and lower range of W2. In the case of significant mobilization pattern during storm events, the highest correlations with β_2 were found with P point sources (R was 0.7). In the case of significant mobilization pattern during storm events, rainfall, BFI and W2 presented strong correlations with β_0 (R were respectively -0.9, -0.6 and 0.7).

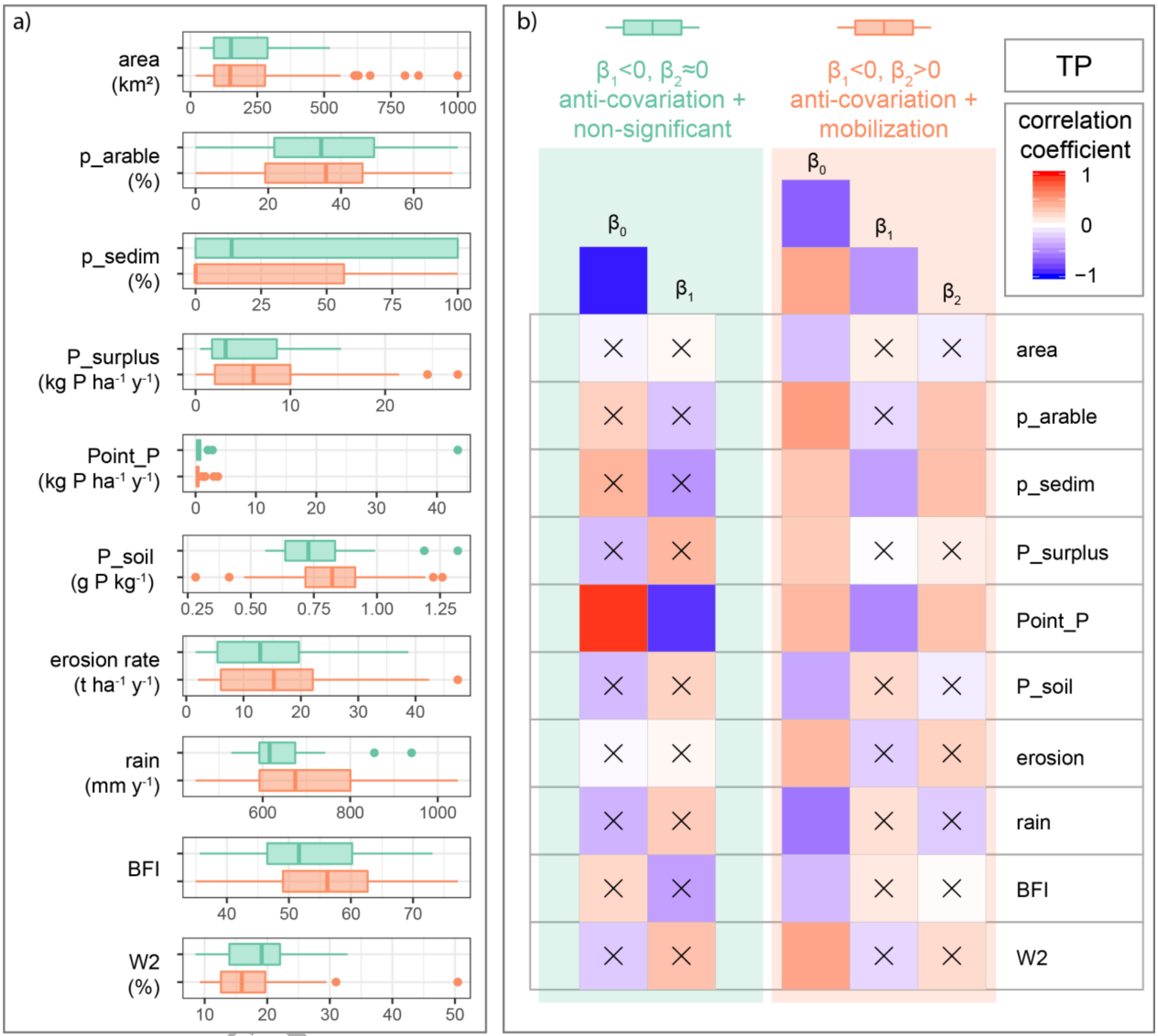

Figure 6. Ranges (a) and correlation matrices (b) between C-Q features (selection based on nRMSE < 200%) characterized by TP background pollution (β_0), seasonal C-Q (β_1), storm C-Q (β_2) and catchment descriptors for the most represented TP-Q types. Black crosses indicate non-significant correlations. Pearson correlation coefficients among catchment descriptors can be found in Table S.1 in the Supplement file.

For SRP (Figure 7), although correlations between SRP C-Q coefficients and catchment descriptors were lower or less significant than the correlation found for the analysis on TP, similar interpretation could be made: β_0 and β_2 were positively linked with point sources, while seasonality β_1 was anti-correlated with point sources. Compared to catchments with a non-significant storm component, catchments with mobilization storm event components presented higher ranges of P surplus, soil P content, and lower erosion rate.

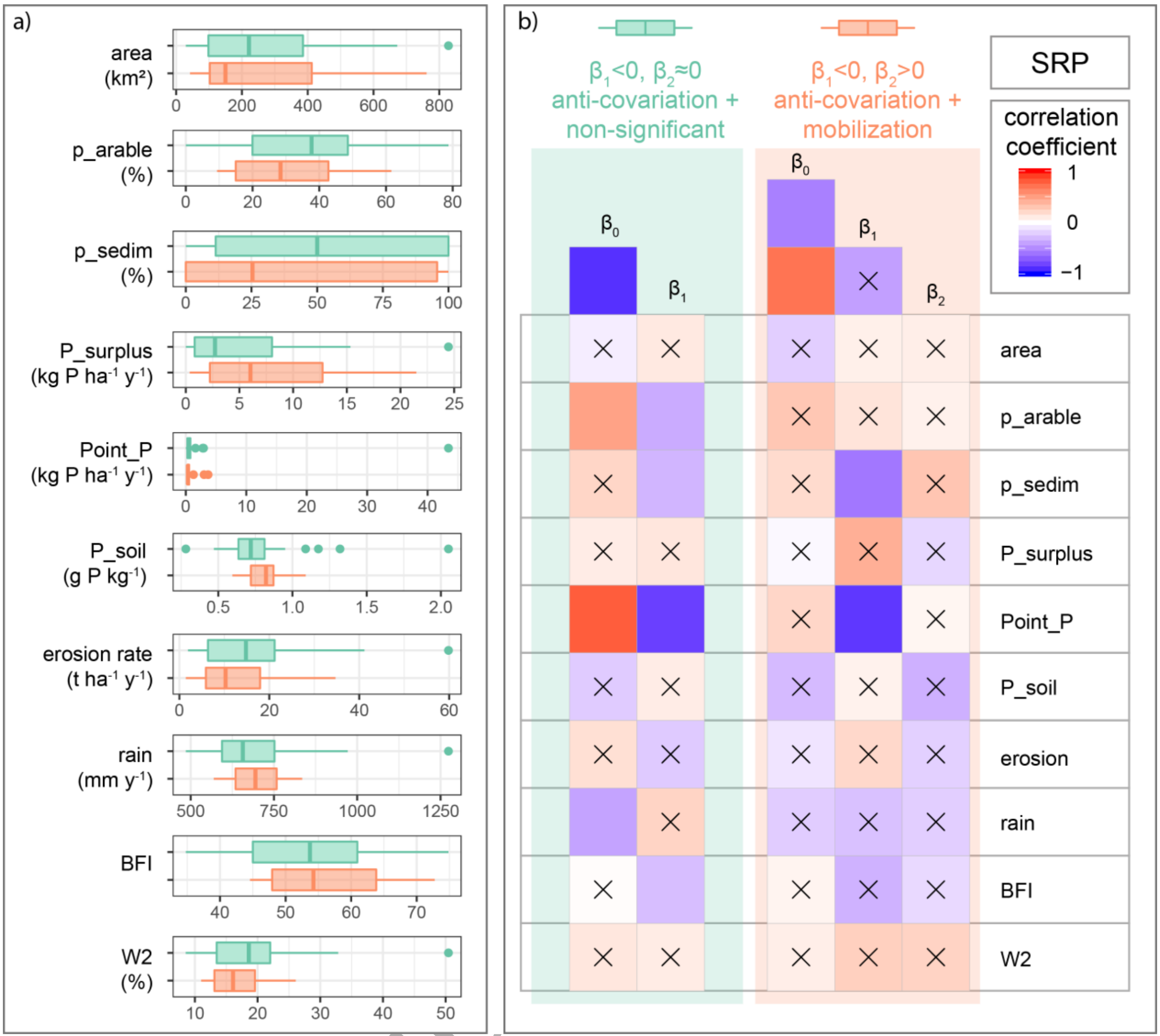

Figure 7. Ranges (a) and correlation matrices (b) between C-Q features (selection based on nRMSE < 200%) characterized by SRP background pollution (β_0), seasonal C-Q (β_1), storm C-Q (β_2) and catchment descriptors for the most represented SRP-Q types. Black crosses indicate non-significant correlations. Pearson correlation coefficients among catchment descriptors can be found in Table S.1 in the Supplement file.

4. Discussion

4.1. Nutrient export regimes at seasonal and storm event scales

The C-$Q_{quick\text{-}slow}$ model revealed different export regimes for nitrate and phosphorus forms at both seasonal and storm event time scales. Nutrient concentration responses to storm events were sometimes opposite to seasonal responses to Q variations, resulting in large dispersion in C-Q plots as is usually observed. This supports the observations from previous studies (Duncan et al., 2017b, 2017a; Li et al., 2019) showing that C-Q relationships may vary across different time scales because the different processes shaping C-Q curves have different temporalities.

Despite the diversity of catchment characteristics in our analysis, only two or three C-Q archetypes were observed among nine theoretical possibilities. This supports the idea developed in Moatar et al. (2017) that the same processes control respectively N and P transfers, across a wide range of environmental conditions.

Seasonal variations displayed consistent patterns across the entire database: we observed positive slow component for nitrate ($\beta_1>0$), and negative slow component for phosphorus ($\beta_1<0$). The processes responsible for seasonal covariation between nitrate and baseflow are either associated with connectivity fluctuation between the stream and the groundwater table (Curie et al., 2011; Duncan et al., 2015; Pinay et al., 1993), or with riparian and in-stream denitrification and biological assimilation (uptake). Disentangling these different processes is challenging because they often occur at the same time: biogeochemical transformations often take place in conditions with high temperature and/or light conditions and long residence times, which coincides with periods of low hydrological connectivity and thus low transport capacity. Opposite seasonality variations between phosphorus concentration and discharge probably result from point sources and their degree of dilution controlling seasonal variations. However, recent studies have found that summer reductive dissolution of iron oxy-hydroxide could also mimic this point-source signal (Dupas et al., 2018; Smolders et al., 2017). It is however noteworthy to remind that in large eutrophic rivers, SRP seasonality can covary with baseflow seasonality due to large algae uptake when low flow coincides with long transit time, optimal light, and temperature conditions (Minaudo et al., 2018, 2015). This particular pattern was not observed in the present study, and we would argue that the selected catchments were too small for algal uptake to become a dominant driver of SRP seasonality.

Storm components for nitrate were in most cases non-significant, suggesting almost unlimited N supply due to large legacy effects (Van Meter and Basu, 2015). This storm component was sometimes negative, indicating dilution effects of diffuse sources by overland flow (Dupas et al., 2016; Fovet et al., 2018). The storm component was sometimes positive, indicating a temporary reconnection between surface and sub-surface waters in catchments likely presenting a vertical gradient of N sources: storms likely flush N stored in the vadose zone (Bende-Michl et al., 2013). For P, when significant, the storm component was in most cases positive, indicating the mobilization of both particulate and dissolved phosphorus. This may occur near agricultural areas with potential interactions with sub-surface water (Dupas et al., 2015c; Gu et al., 2018, 2017; Minaudo et al., 2017), or in-stream by simply re-mobilizing fine sediments stored in the river bed or stored in the river banks (Jarvie et al., 2012; Powers et al., 2016).

4.2. What determines C-Q relationships at the seasonal and storm event scales?

Other studies have looked at potential links between C-Q parameters and catchment descriptors. In most cases, correlations were poor (Diamond and Cohen, 2018; Godsey et al., 2009) but these works evidenced relationships with catchment size, land use, and lithology. In our study, and for all three NO_3^-, TP and SRP, we found strong correlations between C-Q coefficients β_i and readily available catchment variables derived from open-access GIS databases. We found that the magnitude of the background pollution β_0 is determined by diffuse sources intensity (N surplus or p_arable) for nitrate, and by point-sources inputs (P_point) for TP and SRP. Interestingly, and for all three parameters, the absolute magnitude of the seasonal component β_1 was positively correlated with higher background pollution concentration β_0, suggesting that diffuse sources and point sources respectively control seasonal amplitudes of nitrate and phosphorus concentrations. This implies that the most polluted catchments are also the ones with the highest seasonal amplitudes. Different reasons can explain this observation. For nitrate, baseflow concentrations during winter high flow varied more than during summer low flow among the catchments (see Supplementary Figure S.2) arguably because stoichiometric controls during the summer period lead to similar concentrations in different types of catchments, whereas winter concentration better reflects N sources intensity among catchments (Fovet et al., 2018). This supports some recent findings showing that spatial stability for nitrate concentrations is higher over winter months (Dupas et al., 2019b). For phosphorus, we showed that point sources largely control the background pollution in the catchments studied here. Thus, higher loads discharged constantly throughout the year in rivers where flow variations are seasonal is likely to result in limited dilution capacity during low flows, producing large seasonal variations in concentrations

During storm events, we found that the dynamics of both nitrate and phosphorus were linked to both nutrient source indicators and hydrological properties. For instance, we found for NO_3^- that high BFI values, low W2, and low erosion differentiated C-Q dilution patterns from non-significant and mobilization types. This suggested that catchments where shallow groundwater flow contribution dominates are likely to display dilution patterns in storm events due to a sudden increased contribution of young age water (Benettin et al., 2017; Hrachowitz et al., 2016). For TP and SRP, we found that wet catchments with high diffuse P sources and high erosion rates were likely to display a significant mobilization storm event component. This supported the idea that dissolved and particulate P flush during a short term storm event is the consequence of re-mobilization of particles from the river bed or from the streams bank sides (Fox et al., 2016), or the result of an increased connectivity between groundwater and streamflow (Ali et al., 2017; Dupas et al., 2015c; Gu et al., 2017; Rose et al., 2018).

4.3. Potential use of this approach for load estimations

In most countries, water quality monitoring strategies rely on low frequency surveys, typically executed monthly (Dupas et al., 2019b). These surveys are used to determine the water quality status of streams based on a set of simple metrics such as the interannual 90th percentile concentration or interannual fluxes. The validity of these estimations derived from low frequency data has largely been questioned (e.g. Audet et al., 2014; Cassidy and Jordan, 2011; Johnes, 2007; Moatar et al., 2013; Raymond et al., 2013; Rozemeijer et al., 2010), and raises some major management issues where the assessment of water quality indicators is critical. When applicable, the $C\text{-}Q_{quick\text{-}slow}$ model has the potential for interpolating low frequency C time series based on daily Q, and therefor decreases uncertainties in water quality indicators. We illustrated this potential with data from one water quality station located in Brittany where nitrate was monitored daily between 2007 and 2011 (See supplement file). First we subsampled the data to simulate a monthly survey, and then interpolated the subsampled data using the $C\text{-}Q_{quick\text{-}slow}$ model and compared the reconstructed daily concentration and loads to the observations. Results with this example were promising: NO_3^- annual load errors remained under 5% (instead of 10% with a discharge weighted method commonly used in the literature (Moatar and Meybeck, 2005)) and average ± standard deviation errors on monthly loads were 8 ± 6%.

Additionally, the high correlations observed between C-Q coefficients and catchment descriptors suggest that it is possible to predict the most likely C-Q archetype for any catchment, and, then estimate annual and seasonal loads. Applications are numerous and might be the key to empirical estimation of loads in catchments where discharge is measured or can be modelled, but not water quality. Predicting C-Q relationships based on our formulation has to be tested on a large database that covers a large diversity of local contexts in terms of catchment morphology, geology, land use, climate and hydrology.

4.4. Limits and perspectives

Although the C-$Q_{quick\text{-}slow}$ model provided good results for a majority of catchments, C-Q fits were poor for another significant proportion of them. This failure to fit the C-$Q_{quick\text{-}slow}$ model to these catchments means that they do not match one or several of the hypothesis of the model: they could display more complex patterns than what the model can describe, or be too chemostatic for a C-Q model to perform well. For example, the C-$Q_{quick\text{-}slow}$ model does not consider hysteresis effects at both seasonal and storm event times scales, although these are commonly observed (Bieroza and Heathwaite, 2015; Dupas et al., 2015b; Minaudo et al., 2017; Rose et al., 2018). Besides, the slow and quick components defined based on baseflow separation techniques represent in reality more a separation of responses in time to streamflow variations than a water source separation (McDonnell and Beven, 2014). In the particular case of nitrate, we assumed that a concentration gradient across the subsurface-to-groundwater layer would be enough to explain slow and quick variations in time, but a non-significant quick component in 52% cases in our study may indicate a conceptual limitation of our model. Indeed, the C-$Q_{quick\text{-}slow}$ model does not allow storm event responses to vary across seasons, although several studies have documented these variations (Dupas et al., 2016; Fovet et al., 2018). In our approach, the magnitude of C variations among events as a linear function of log-transformed quickflow variations, but the sign of the C-Q coefficient β_2 or its intensity across a succession of similar Q events could not change. Thus, the C-Q relationship could only be poorly adjusted to the observations for catchments where the behavior for summer storms is for instance inverted compared to the behavior for winter storms, or where C supply is easily depleted. An interaction term between the two temporal scales could be added to the equation, but this would result in an additional coefficient that would increase the risk of overfitting the model. Finally, we assumed in this study that grab samples could represent a daily mean concentration, which is not verified in several studies in small catchments showing large sub-daily variations (Halliday et al., 2015; Minaudo et al., 2017; Rode et al., 2016), thus increasing uncertainty of the model calibration data. Although this certainly limits the use of the C-$Q_{quick\text{-}slow}$ model with grab sample data in small and hydrologically reactive catchments, the model could be tested with sub-daily probe data where they exist.

5. Conclusions

The C-$Q_{quick\text{-}slow}$ model is a new C-Q model that considers the possibility for different C-Q relationships at the storm event scale and at the seasonal scale. Results showed that the slopes of C-Q relationships can be different or even opposite at storm event time and seasonal scales, which explains a large part of the dispersion commonly observed in C-Q plots.

We showed that NO_3^--Q relationships at the seasonal scale were in 75% cases positive and relationships in storms were either showing dilution pattern (24% cases), a non-significant pattern (50%), or a mobilization pattern (12%). TP and SRP relationships with Q at the seasonal scale were almost systematically negative (95%), and patterns during storm events were in most cases showing a mobilization for TP (77%) or were non-significant for SRP (69%). We have linked the different C-Q relationships with catchment descriptors and found that indicators of diffuse sources loads determined NO_3^- seasonal amplitudes, and hydrological drivers could explain the behavior during storms. In contrast, point sources determined P seasonal amplitudes, and diffuse sources combined with erosion rate likely controlled P behavior during storm events. The C-$Q_{quick-slow}$ model has the potential to improve nutrient load estimations because of the good predictability of appropriate C-Q archetypes and the possibility to interpolate low frequency concentration data to a daily frequency.

Author contributions

The concept for this paper emerged during discussions between C.M. and R.D. C.M. downloaded the data and ran the GIS, model and statistical analysis. C.M. wrote the manuscript with input from all the co-authors.

Acknowledgements

This work was funded by the "Agence Française pour la Biodiversité (AFB)", the French National Agency for Biodiversity. The authors are grateful to the French Water Basin Agencies and their partners who contributed to the water quality data acquisition. Water quality and discharge data used in this study are available from public repositories at http://osur.eau-loirebretagne.fr/ and http://hydro.eaufrance.fr/.

References

Abbott, B.W., Moatar, F., Gauthier, O., Fovet, O., Antoine, V., Ragueneau, O., 2018. Trends and seasonality of river nutrients in agricultural catchments: 18 years of weekly citizen science in France. Sci. Total Environ. 624, 845–858. https://doi.org/10.1016/j.scitotenv.2017.12.176

Ali, G., Wilson, H., Elliott, J., Penner, A., Haque, A., Ross, C., Rabie, M., 2017. Phosphorus export dynamics and hydrobiogeochemical controls across gradients of scale, topography and human impact. Hydrol. Process. 31, 3130–3145. https://doi.org/10.1002/hyp.11258

Ameli, A.A., Beven, K., Erlandsson, M., Creed, I.F., McDonnell, J.J., Bishop, K., 2017. Primary weathering rates, water transit times, and concentration-discharge relations: A theoretical analysis for the critical zone. Water Resour. Res. 53, 942–960. https://doi.org/10.1002/2016WR019448

Audet, J., Martinsen, L., Hasler, B., De Jonge, H., Karydi, E., Ovesen, N.B., Kronvang, B., 2014. Comparison of sampling methodologies for nutrient monitoring in streams: Uncertainties, costs and implications for mitigation. Hydrol. Earth Syst. Sci. 18, 4721–4731. https://doi.org/10.5194/hess-18-4721-2014

Basu, N.B., Thompson, S.E., Rao, P.S.C., 2011. Hydrologic and biogeochemical functioning of intensively managed catchments: A synthesis of top-down analyses. Water Resour. Res. 47, n/a-n/a. https://doi.org/10.1029/2011WR010800

Bende-Michl, U., Verburg, K., Cresswell, H.P., 2013. High-frequency nutrient monitoring to infer seasonal patterns in catchment source availability, mobilisation and delivery. Environ. Monit. Assess. 185, 9191–9219. https://doi.org/10.1007/s10661-013-3246-8

Benettin, P., Bailey, S.W., Rinaldo, A., Likens, G.E., McGuire, K.J., Botter, G., 2017. Young runoff fractions control streamwater age and solute concentration dynamics. Hydrol. Process. 31, 2982–2986. https://doi.org/10.1002/hyp.11243

Bieroza, M., Heathwaite, A.L., 2015. Seasonal variation in phosphorus concentration–discharge hysteresis inferred from high-frequency in situ monitoring. J. Hydrol. 524, 333–347. https://doi.org/10.1016/j.jhydrol.2015.02.036

Bieroza, M.Z., Heathwaite, A.L., 2016. Unravelling organic matter and nutrient biogeochemistry in groundwater-fed rivers under baseflow conditions: Uncertainty in in situ high-frequency analysis. Sci. Total Environ. 572, 1520–1533. https://doi.org/10.1016/j.scitotenv.2016.02.046

Bieroza, M.Z., Heathwaite, A.L., Bechmann, M., Kyllmar, K., Jordan, P., 2018. The concentration-discharge slope as a tool for water quality management. Sci. Total Environ. 630, 738–749. https://doi.org/10.1016/j.scitotenv.2018.02.256

Bol, R., Gruau, G., Mellander, P.-E., Dupas, R., Bechmann, M., Skarbøvik, E., Bieroza, M., Djodjic, F., Glendell, M., Jordan, P., Van der Grift, B., Rode, M., Smolders, E., Verbeeck, M., Gu, S., Klumpp, E., Pohle, I., Fresne, M., Gascuel-Odoux, C., 2018. Challenges of Reducing Phosphorus Based Water Eutrophication in the Agricultural Landscapes of Northwest Europe. Front. Mar. Sci. 5, 0–16. https://doi.org/10.3389/fmars.2018.00276

Cassidy, R., Jordan, P., 2011. Limitations of instantaneous water quality sampling in surface-water catchments: Comparison with near-continuous phosphorus time-series data. J.

Hydrol. 405, 182–193. https://doi.org/10.1016/j.jhydrol.2011.05.020

Cerdan, O., Govers, G., Le Bissonnais, Y., Van Oost, K., Poesen, J., Saby, N., Gobin, A., Vacca, A., Quinton, J., Auerswald, K., Klik, A., Kwaad, F.J.P.M., Raclot, D., Ionita, I., Rejman, J., Rousseva, S., Muxart, T., Roxo, M.J., Dostal, T., 2010. Rates and spatial variations of soil erosion in Europe: A study based on erosion plot data. Geomorphology 122, 167–177. https://doi.org/10.1016/j.geomorph.2010.06.011

CLC2006, 2006. Corine Land Cover. https://land.copernicus.eu/pan-european/corine-land-cover.

Curie, F., Ducharne, A., Bendjoudi, H., Billen, G., 2011. Spatialization of denitrification by river corridors in regional-scale watersheds: Case study of the Seine river basin. Phys. Chem. Earth 36, 530–538. https://doi.org/10.1016/j.pce.2009.02.004

Delmas, M., Saby, N., Arrouays, D., Dupas, R., Lemercier, B., Pellerin, S., Gascuel-Odoux, C., 2015. Explaining and mapping total phosphorus content in French topsoils. Soil Use Manag. 31, 259–269. https://doi.org/10.1111/sum.12192

Diamond, J.S., Cohen, M.J., 2018. Complex patterns of catchment solute-discharge relationships for coastal plain rivers. Hydrol. Process. 32, 388–401. https://doi.org/10.1002/hyp.11424

Doublet, S., Le Gall, P., 2013. NOPOLU-Agri. Outil de spatialisation des pressions de l’agriculture. Méthodologie et résultats pour les surplus d’azote et les émissions des gaz à effet de serre. Campagne 2010-2011.

Duncan, J.M., Band, L.E., Groffman, P.M., 2017a. Variable nitrate concentration–discharge relationships in a forested watershed. Hydrol. Process. 31, 1817–1824. https://doi.org/10.1002/hyp.11136

Duncan, J.M., Band, L.E., Groffman, P.M., Bernhardt, E.S., 2015. Mechanisms driving the seasonality of catchment scale nitrate export: Evidence for riparian ecohydrologic controls. Water Resour. Res. 51, 3982–3997. https://doi.org/10.1002/2015WR016937

Duncan, J.M., Welty, C., Kemper, J.T., Groffman, P.M., Band, L.E., 2017b. Dynamics of nitrate concentration-discharge patterns in an urban watershed. Water Resour. Res. 53, 7349–7365. https://doi.org/10.1002/2017WR020500

Dupas, R., Abbott, B.W., Minaudo, C., Fovet, O., 2019a. Distribution of landscape units within catchments influences nutrient export dynamics. Front. Environ. Sci. 7, 43. https://doi.org/10.3389/FENVS.2019.00043

Dupas, R., Delmas, M., Dorioz, J., Garnier, J., 2015a. Assessing the impact of agricultural pressures on N and P loads and eutrophication risk. Ecol. Indic. 48, 396–407. https://doi.org/10.1016/j.ecolind.2014.08.007

Dupas, R., Gascuel-Odoux, C., Gilliet, N., Grimaldi, C., Gruau, G., 2015b. Distinct export dynamics for dissolved and particulate phosphorus reveal independent transport mechanisms in an arable headwater catchment. Hydrol. Process. 29, 3162–3178. https://doi.org/10.1002/hyp.10432

Dupas, R., Gruau, G., Gu, S., Humbert, G., Jaffrézic, A., Gascuel-Odoux, C., 2015c. Groundwater control of biogeochemical processes causing phosphorus release from riparian wetlands. Water Res. 84, 307–314. https://doi.org/10.1016/j.watres.2015.07.048

Dupas, R., Jomaa, S., Musolff, A., Borchardt, D., Rode, M., 2016. Disentangling the influence of hydroclimatic patterns and agricultural management on river nitrate dynamics from sub-hourly to decadal time scales. Sci. Total Environ. 571, 791–800. https://doi.org/10.1016/j.scitotenv.2016.07.053

Dupas, R., Minaudo, C., Abbott, B.W., 2019b. Stability of spatial patterns in water chemistry across temperate ecoregions. Environ. Res. Lett. https://doi.org/10.1088/1748-9326/ab24f4

Dupas, R., Musolff, A., Jawitz, J.W., Rao, P.S.C., Jäger, C.G., Fleckenstein, J.H., Rode, M., Borchardt, D., 2017. Carbon and nutrient export regimes from headwater catchments to downstream reaches. Biogeosciences 14, 4391–4407. https://doi.org/10.5194/bg-14-4391-2017

Dupas, R., Tittel, J., Jordan, P., Musolff, A., Rode, M., 2018. Non-domestic phosphorus release in rivers during low-flow: Mechanisms and implications for sources identification. J. Hydrol. 560, 141–149. https://doi.org/10.1016/j.jhydrol.2018.03.023

Eckhardt, K., 2008. A comparison of baseflow indices, which were calculated with seven different baseflow separation methods. J. Hydrol. 352, 168–173. https://doi.org/10.1016/j.jhydrol.2008.01.005

Fovet, O., Humbert, G., Dupas, R., Gascuel-Odoux, C., Gruau, G., Jaffrezic, A., Thelusma, G., Faucheux, M., Gilliet, N., Hamon, Y., Grimaldi, C., 2018. Seasonal variability of stream water quality response to storm events captured using high-frequency and multi-parameter data. J. Hydrol. 559, 282–293. https://doi.org/10.1016/j.jhydrol.2018.02.040

Fox, G.A., Purvis, R.A., Penn, C.J., 2016. Streambanks: A net source of sediment and phosphorus to streams and rivers. J. Environ. Manage. 181, 602–614. https://doi.org/10.1016/j.jenvman.2016.06.071

Godsey, S.E., Kirchner, J.W., Clow, D.W., 2009. Concentration–discharge relationships reflect chemostatic characteristics of US catchments. Hydrol. Process. 23, 1844–1864. https://doi.org/10.1002/hyp.7315

Gu, S., Gruau, G., Dupas, R., Rumpel, C., Crème, A., Fovet, O., Gascuel-Odoux, C., Jeanneau, L., Humbert, G., Petitjean, P., 2017. Release of dissolved phosphorus from riparian wetlands: Evidence for complex interactions among hydroclimate variability, topography and soil properties. Sci. Total Environ. 598, 421–431. https://doi.org/10.1016/j.scitotenv.2017.04.028

Gu, S., Gruau, G., Malique, F., Dupas, R., Petitjean, P., Gascuel-Odoux, C., 2018. Drying/rewetting cycles stimulate release of colloidal-bound phosphorus in riparian soils. Geoderma 321, 32–41. https://doi.org/10.1016/j.geoderma.2018.01.015

Halliday, S.J., Skeffington, R. a., Wade, A.J., Bowes, M.J., Gozzard, E., Newman, J.R., Loewenthal, M., Palmer-Felgate, E.J., Jarvie, H.P., 2015. High-frequency water quality monitoring in an urban catchment: hydrochemical dynamics, primary production and implications for the Water Framework Directive. Hydrol. Process. 29, 3388–3407. https://doi.org/10.1002/hyp.10453

Hipel, K.W., McLeod, A.I., 2005. Time Series Modelling of Water Resources and Environmental Systems. http://www.stats.uwo.ca/faculty/aim/1994Book/.

Hirsch, R.M., 2014. Large Biases in Regression-Based Constituent Flux Estimates: Causes and Diagnostic Tools. JAWRA J. Am. Water Resour. Assoc. 50, 1401–1424. https://doi.org/10.1111/jawr.12195

Hrachowitz, M., Benettin, P., Breukelen, B.M. Van, Fovet, O., Howden, N.J.K., Ruiz, L., Velde, Y. Van Der, Wade, A.J., 2016. Transit times - the link between hydrology and water quality at the catchment scale. WIREs Water 3, 629–657. https://doi.org/10.1002/wat2.1155

Jarvie, H.P., Sharpley, A.N., Scott, J.T., Haggard, B.E., Bowes, M.J., Massey, L.B., 2012. Within-River Phosphorus Retention: Accounting for a Missing Piece in the Watershed Phosphorus Puzzle. Environ. Sci. Technol. 46, 13284–13292. https://doi.org/10.1021/es303562y

Jawitz, J.W., Mitchell, J., 2011. Temporal inequality in catchment discharge and solute export. Water Resour. Res. 47, n/a-n/a. https://doi.org/10.1029/2010WR010197

Johnes, P.J., 2007. Uncertainties in annual riverine phosphorus load estimation: Impact of load estimation methodology, sampling frequency, baseflow index and catchment population density. J. Hydrol. 332, 241–258. https://doi.org/10.1016/j.jhydrol.2006.07.006

Kim, H., Dietrich, W.E., Thurnhoffer, B.M., Bishop, J.K.B., Fung, I.Y., 2017. Controls on solute concentration-discharge relationships revealed by simultaneous hydrochemistry observations of hillslope runoff and stream flow: The importance of critical zone structure. Water Resour. Res. 1–20. https://doi.org/10.1002/2016WR019722

Koenig, L.E., Shattuck, M.D., Snyder, L.E., Potter, J.D., McDowell, W.H., 2017. Deconstructing the Effects of Flow on DOC, Nitrate, and Major Ion Interactions Using a High-Frequency Aquatic Sensor Network. Water Resour. Res. 655–673. https://doi.org/10.1002/2017WR020739

Li, W., Liu, H., Zhai, L., Yen, H., Hu, W., Lei, Q., Stewart, R.J., Guo, S., Ren, T., 2019. Evaluation of concentration-discharge dynamics and nitrogen export on anthropogenic inputs and stormflow across alternative time-scales. Ecol. Indic. 98, 879–887. https://doi.org/10.1016/j.ecolind.2018.11.057

LITHO, 2008. dataset - http://www.geocatalogue.fr/Detail.do?id=6388.

Lyne, V.D., Hollick, M., 1979. Stochastic time-variable rainfall-runoff modelling. Inst. Eng. Aust. Natl. Conf. 89–93.

McDonnell, J.J., Beven, K., 2014. Debates-The future of hydrological sciences: A (common) path forward? A call to action aimed at understanding velocities, celerities and residence time distributions of the headwater hydrograph. Water Resour. Res. 50, 5342–5350. https://doi.org/10.1002/2013WR015141

Minaudo, C., Curie, F., Jullian, Y., Gassama, N., Moatar, F., 2018. QUAL-NET, a high temporal-resolution eutrophication model for large hydrographic networks. Biogeosciences 15, 2251–2269. https://doi.org/10.5194/bg-15-2251-2018

Minaudo, C., Dupas, R., Gascuel-Odoux, C., Fovet, O., Mellander, P.-E., Jordan, P., Shore, M., Moatar, F., 2017. Nonlinear empirical modeling to estimate phosphorus exports using continuous records of turbidity and discharge. Water Resour. Res. 53, 7590–7606. https://doi.org/10.1002/2017WR020590

Minaudo, C., Meybeck, M., Moatar, F., Gassama, N., Curie, F., 2015. Eutrophication mitigation in rivers: 30 years of trends in spatial and seasonal patterns of biogeochemistry of the Loire River (1980–2012). Biogeosciences 12, 2549–2563. https://doi.org/10.5194/bg-12-2549-2015

Moatar, F., Abbott, B.W., Minaudo, C., Curie, F., Pinay, G., 2017. Elemental properties, hydrology, and biology interact to shape concentration-discharge curves for carbon, nutrients, sediment, and major ions. Water Resour. Res. 53, 1–18. https://doi.org/10.1002/2016WR019635

Moatar, F., Meybeck, M., 2005. Compared performances of different algorithms for estimating annual nutrient loads discharged by the eutrophic River Loire. Hydrol. Process. 19, 429–444. https://doi.org/10.1002/hyp.5541

Moatar, F., Meybeck, M., Raymond, S., Birgand, F., Curie, F., 2013. River flux uncertainties predicted by hydrological variability and riverine material behaviour. Hydrol. Process. 27, 3535–3546. https://doi.org/10.1002/hyp.9464

Musolff, A., Fleckenstein, J.H., Rao, P.S.C., Jawitz, J.W., 2017. Emergent archetype patterns of coupled hydrologic and biogeochemical responses in catchments. Geophys. Res. Lett. 44, 4143–4151. https://doi.org/10.1002/2017GL072630

Musolff, A., Schmidt, C., Rode, M., Lischeid, G., Weise, S.M., Fleckenstein, J.H., 2016. Groundwater head controls nitrate export from an agricultural lowland catchment. Adv. Water Resour. 96, 95–107. https://doi.org/10.1016/j.advwatres.2016.07.003

Musolff, A., Schmidt, C., Selle, B., Fleckenstein, J.H., 2015. Catchment controls on solute export. Adv. Water Resour. 86, 133–146. https://doi.org/10.1016/j.advwatres.2015.09.026

Nathan, R.J., McMahon, T.A., 1990. Evaluation of automated techniques for base flow and recession analyses. Water Resour. Res. 26, 1465–1473. https://doi.org/10.1029/WR026i007p01465

Pinay, G., Roques, L., Fabre, A., 1993. Spatial and temporal patterns of denitrification in a riparian forest. J. Appl. Ecol. 30, 581–591. https://doi.org/10.2307/2404238

Powers, S.M., Bruulsema, T.W., Burt, T.P., Chan, N.I., Elser, J.J., Haygarth, P.M., Howden, N.J.K., Jarvie, H.P., Lyu, Y., Peterson, H.M., Sharpley, A.N., Shen, J., Worrall, F., Zhang, F., 2016. Long-term accumulation and transport of anthropogenic phosphorus in three river basins. Nat. Geosci. 9, 353–356. https://doi.org/10.1038/ngeo2693

Quintana-Segui, P., Le Moigne, P., Durand, Y., Martin, E., Habets, F., Baillon, M., Canellas, C., Franchisteguy, L., Morel, S., 2008. Analysis of near-surface atmospheric variables: Validation of the SAFRAN analysis over France. J. Appl. Meteorol. Climatol. 47, 92–107. https://doi.org/10.1175/2007JAMC1636.1

R Core Team, 2016. R Core Team (2016). R: A language and environment for statistical computing. R Foundation for Statistical Computing, Vienna, Austria.

Raymond, S., Moatar, F., Meybeck, M., Bustillo, V., 2013. Choosing methods for estimating dissolved and particulate riverine fluxes from monthly sampling. Hydrol. Sci. J. 58, 1326–1339. https://doi.org/10.1080/02626667.2013.814915

Rode, M., Wade, A.J., Cohen, M.J., Hensley, R.T., Bowes, M.J., Kirchner, J.W., Arhonditsis, G.B., Jordan, P., Kronvang, B., Halliday, S.J., Skeffington, R.A., Rozemeijer, J.C., Aubert, A.H., Rinke, K., Jomaa, S., 2016. Sensors in the Stream: The High-Frequency

Wave of the Present. Environ. Sci. Technol. 50, 10297–10307. https://doi.org/10.1021/acs.est.6b02155

Rose, L.A., Karwan, D.L., Godsey, S.E., 2018. Concentration-discharge relationships describe solute and sediment mobilization, reaction, and transport at event and longer timescales. Hydrol. Process. 1–16. https://doi.org/10.1002/hyp.13235

Rozemeijer, J.C., Van Der Velde, Y., Van Geer, F.C., De Rooij, G.H., Torfs, P.J.J.F., Broers, H.P., 2010. Improving load estimates for NO3 and P in surface waters by characterizing the concentration response to rainfall events. Environ. Sci. Technol. 44, 6305–6312. https://doi.org/10.1021/es101252e

Smolders, E., Baetens, E., Verbeeck, M., Nawara, S., Diels, J., Verdievel, M., Peeters, B., De Cooman, W., Baken, S., 2017. Internal Loading and Redox Cycling of Sediment Iron Explain Reactive Phosphorus Concentrations in Lowland Rivers. Environ. Sci. Technol. 51, 2584–2592. https://doi.org/10.1021/acs.est.6b04337

Snoubra, B., 2013. Les surplus d’azote et les gaz à effet de serre de l’activité agricole en France métropolitaine en 2010. Chiffres Stat. Serv. l’observation des Stat. Commis. général au développement durable 448.

Thompson, S.E., Basu, N.B., Lascurain, J., Aubeneau, A., Rao, P.S.C., 2011. Relative dominance of hydrologic versus biogeochemical factors on solute export across impact gradients. Water Resour. Res. 47, 1–20. https://doi.org/10.1029/2010WR009605

Tiwari, T., Lidman, F., Laudon, H., Lidberg, W., Ågren, A.M., 2017. GIS-based prediction of stream chemistry using landscape composition, wet areas, and hydrological flow pathways. J. Geophys. Res. Biogeosciences 122, 65–79. https://doi.org/10.1002/2016JG003399

Underwood, K.L., Rizzo, D.M., Schroth, A.W., Dewoolkar, M.M., 2017. Evaluating Spatial Variability in Sediment and Phosphorus Concentration-Discharge Relationships Using Bayesian Inference and Self-Organizing Maps. Water Resour. Res. 53, 10293–10316. https://doi.org/10.1002/2017WR021353

Van Meter, K.J., Basu, N.B., 2015. Catchment legacies and time lags: A parsimonious watershed model to predict the effects of legacy storage on nitrogen export. PLoS One 10, 1–22. https://doi.org/10.1371/journal.pone.0125971

Williams, M.R., King, K.W., Baker, D.B., Johnson, L.T., Smith, D.R., Fausey, N.R., 2016. Hydrologic and biogeochemical controls on phosphorus export from Western Lake Erie tributaries. J. Great Lakes Res. 42, 1403–1411. https://doi.org/10.1016/j.jglr.2016.09.009

Zhang, Q., Ball, W.P., 2017. Improving riverine constituent concentration and flux estimation by accounting for antecedent discharge conditions. J. Hydrol. 547, 387–402. https://doi.org/10.1016/j.jhydrol.2016.12.052

Zhang, Q., Brady, D.C., Boynton, W.R., Ball, W.P., 2015. Long-term trends of nutrients and sediment from the nontidal Chesapeake watershed. J. Am. Water Resour. Assoc. 1–22. https://doi.org/10.1111/1752-1688.12327

Zhang, Q., Harman, C.J., Ball, W.P., 2016. An improved method for interpretation of riverine concentration-discharge relationships indicates long-term shifts in reservoir sediment trapping. Geophys. Res. Lett. 43, 10,215-10,224. https://doi.org/10.1002/2016GL069945